Journal of Sound and Vibration 329 (2010) 4251–4265

Contents lists available at ScienceDirect

Journal of Sound and Vibration

journal homepage: www.elsevier.com/locate/jsvi

# Nonlinear vibration of viscoelastic sandwich beams by the harmonic balance and finite element methods

N. Jacques [a,*], E.M. Daya [b], M. Potier-Ferry [b]

[a] Laboratoire Brestois de Mécanique et des Systèmes, ENSIETA/Université de Bretagne Occidentale/ENIB, 2 rue François Verny, 29806 Brest Cedex 9, France
[b] Laboratoire de Physique et Mécanique des Matériaux (LPMM), FRE CNRS 3236, Université Paul Verlaine-Metz, Ile du Saulcy, 57045 Metz Cedex 01, France

ARTICLE INFO

*Article history:*
Received 24 September 2008
Received in revised form
20 April 2010
Accepted 20 April 2010
Handling Editor: A.V. Metrikine
Available online 18 May 2010

ABSTRACT

This paper deals with geometrically nonlinear vibrations of sandwich beams with viscoelastic materials. For this purpose, a new finite element formulation has been developed, in which a zig-zag model is used to describe the displacement field. The viscoelastic behaviour is handled by using hereditary integrals and their relationships with complex moduli. An efficient solution procedure based on the harmonic balance method is also developed. To demonstrate its abilities, various problems of nonlinear vibrations of sandwich beams are considered. First, the results derived from the proposed approach are compared with those of nonlinear dynamic analyses using direct time integration and to experimental data. Then, the influence of the vibration amplitude on the damping properties of sandwich beams is investigated. The effect of an initial axial strain is also examined.



## 1. Introduction

Control of noise and vibration is an important issue in structural engineering. Viscoelastic materials have long been recognized as excellent vibration dampers; viscoelastic coatings and tapes have frequently been applied to control flexural vibration. If a thin viscoelastic layer is sandwiched between two stiff elastic layers, even greater damping can be obtained with only a slight increase in weight. Due to the low stiffness of the viscoelastic material, the sandwich construction induces a shearing motion in the core layer, leading to very effective damping properties [1].

Considerable theoretical and experimental work has been done on the linear dynamic behaviour of sandwich structures with viscoelastic layers. In order to predict the dynamic response and the damping properties of these structures, it is necessary to accurately describe the shear strain in the viscoelastic layers. For this reason, equivalent single-layer theories, such as the classical laminate theory and the first-order shear deformation theory, are generally inadequate [2]. More refined kinematic models devoted to sandwich structures have therefore been proposed. Fundamental early work was conducted by Kerwin [1], who suggested a formula for estimating the loss factor of three-layer sandwich beams. Several later analytical studies were dedicated to simple structures [3–7], and finite element computations have also been proposed to deal with engineering problems in structural dynamics [8–13]. A common feature of the theories underpinning these works is to assume a displacement field for each layer. Governing equations are obtained by looking at the equilibrium of each layer, together with the interface conditions. This kind of model is known as a layerwise or a zig-zag model.

* Corresponding author. Tel.: +33 2 98 34 89 36; fax: +33 2 98 34 87 30.
*E-mail address:* nicolas.jacques@ensieta.fr (N. Jacques).

0022-460X/$ - see front matter © 2010 Elsevier Ltd. All rights reserved.
doi:10.1016/j.jsv.2010.04.021

When structures undergo severe dynamic loadings, large-amplitude vibrations arise and geometric nonlinearity may induce a dynamic behaviour that is significantly different from the one predicted by linear structural theories. It is well known, for example, that resonance frequencies and mode shapes are generally amplitude-dependent. The study of the nonlinear vibration of structures has attracted many researchers, but only a few papers have dealt with sandwich structures. Kovac et al. [14], Hyer et al. [15], and Daya et al. [16] performed analytical studies of the nonlinear vibration of sandwich beams. In these studies, frequency–amplitude relationships were obtained by means of the one-mode Galerkin's procedure and the harmonic balance method. The studies of Kovac et al. [14] and Hyer et al. [15] also included experiments, which produced reasonable agreement with the theory. Nevertheless, because these analytical models are based on the one-mode Galerkin's method, they are likely to provide accurate results only near a resonance frequency. Moreover, the effect of large vibration amplitudes on the mode shape is disregarded. In order to overcome these limitations, numerical techniques such as finite elements must be used. Direct time-integration analyses using, for instance, Newmark's method can be applied to compute the nonlinear dynamic response of structures with viscoelastic parts [17,18]. However, if the steady-state response to harmonic excitation is sought, time domain techniques have high computational requirements. Consequently, these techniques are not very appropriate for investigating the forced response within a large range of excitation frequencies. For the class of problems where the motion can be assumed to be periodic in time, frequency-domain methods such as the harmonic balance method allow us to achieve shorter computation times. In the case of homogeneous beams and plates, the combined use of the harmonic balance and finite element methods has proved to be a versatile and efficient technique for computing the response in the frequency domain [19–23]. Iu et al. [24] proposed a numerical model for the nonlinear vibration of multilayer sandwich beams. In their approach, the structure is discretised in space by the finite element method, and the periodic solutions of the resulting set of ordinary differential equations are obtained by using the harmonic balance method. Iu and Cheung [25] applied a similar technique to study the nonlinear vibration of sandwich plates. Nevertheless, in these papers [24,25], only viscous damping (in which damping forces are proportional to the absolute velocity) is taken into account. This kind of model is generally unable to accurately describe the energy dissipation behaviour of real structural viscoelastic materials such as plastics or polymers.

From the reviewed works, it appears that it remains challenging to develop an efficient frequency-domain method that is able to handle both viscoelasticity and geometric nonlinearity. Designing such a method is the main aim of this paper. Attention is focused on three-layer sandwich beams with a viscoelastic core, but the proposed methodology can be applied to more complex structures as well. In our approach, the constitutive properties of the viscoelastic core are handled by using hereditary integrals and their relationships with complex moduli. The solution procedure is based on the harmonic balance technique and the finite element method. Here, the harmonic balance method is used to obtain an approximate variational equation of motion in the frequency domain. Then, a finite element approximation in space is introduced. The developed finite element method has been implemented in the commercial software ABAQUS. Comprehensive numerical tests for the forced response of sandwich beams are reported. In order to provide a validation of the proposed method, the results are compared with those of fully nonlinear computations using direct time integration and with experimental data. Also, results about the effect of large vibration amplitudes on the damping properties of sandwich beams are presented. Finally, the nonlinear vibration of a pre-stressed beam is analysed.

## 2. Governing equations

We focus on three-layer symmetrical beams with a viscoelastic core. $L$ is the length of the beam; $h_f$ and $h_c$ are the thicknesses of the face and core layers, respectively; and $x$ and $z$ are the axial and transverse coordinates, respectively. The mid-plane of the beam is set to coincide with the origin of the $z$-axis.

A layerwise model, in which the face layers are assumed to behave as Euler–Bernoulli beams and the core layer is modelled according to Timoshenko's theory, is used to construct the displacement field. The accuracy of this formulation in the case of sandwich beams with soft cores has been established in several studies [2,26,27]. Moreover, the following hypotheses are formed:

- The three layers are perfectly bonded and in a plane stress state.
- The out-of-plane displacement does not depend on the transverse coordinate.
- The face layers are isotropic elastic. In addition, the two faces have the same Young's modulus.
- The core layer has an isotropic frequency-dependent viscoelastic behaviour. However, the Poisson ratio is constant. This assumption, often adopted in the literature, implies that the shear and Young's moduli are proportional.

### 2.1. Displacements and strains

The longitudinal displacement $U_i$ at any point in the elastic layers is given by

$$U_i(x,z,t) = u_i(x,t) - (z - z_i)\frac{\partial w(x,t)}{\partial x}, \quad i = 1, 3, \tag{1}$$

where $z_i$ and $u_i(x,t)$ are the $z$-coordinate and the axial displacement of the mid-plane of the $i$th layer, respectively, and $w$ is the transverse displacement.

The axial displacement $U_2$ of a point in the central layer can be written as

$$U_2(x,z,t) = u(x,t) + z\beta(x,t), \tag{2}$$

where $u(x,t)$ is the axial displacement of a point on the plane $z=0$ and $\beta(x,t)$ is the rotation of the normal to the sandwich mid-plane.

The following nonlinear strain–displacement relationships, which account for small strains and moderate rotations, are used:

$$\begin{aligned}
\varepsilon_i(x,z,t) &= \frac{\partial u_i(x,t)}{\partial x} + \frac{1}{2}\left(\frac{\partial w(x,t)}{\partial x}\right)^2 - (z-z_i)\frac{\partial^2 w(x,t)}{\partial x^2}, \quad i = 1, 3,\\
\varepsilon_2(x,z,t) &= \frac{\partial u(x,t)}{\partial x} + \frac{1}{2}\left(\frac{\partial w(x,t)}{\partial x}\right)^2 + z\frac{\partial \beta(x,t)}{\partial x},\\
\gamma_2(x,t) &= \frac{\partial w(x,t)}{\partial x} + \beta(x,t),
\end{aligned} \tag{3}$$

where $\varepsilon_i$ is the axial strain in the $i$th layer and $\gamma_2$ is the shear strain in the core.

Assuming perfect bonding between layers, the axial displacements of the face layers may be written as a function of the above defined variables $u$ and $\beta$:

$$\begin{aligned}
u_1(x,t) &= u(x,t) + \left(\frac{h_c}{2}\beta(x,t) - \frac{h_f}{2}\frac{\partial w(x,t)}{\partial x}\right),\\
u_3(x,t) &= u(x,t) - \left(\frac{h_c}{2}\beta(x,t) - \frac{h_f}{2}\frac{\partial w(x,t)}{\partial x}\right).
\end{aligned} \tag{4}$$

### 2.2. Constitutive relations

The expressions of the axial forces $N_i$ and the bending moments $M_i$ in the two elastic faces can be written as

$$\begin{aligned}
N_i &= E_f S_f \left(\frac{\partial u_i}{\partial x} + \frac{1}{2}\left(\frac{\partial w}{\partial x}\right)^2\right),\\
M_i &= -E_f I_f \frac{\partial^2 w}{\partial x^2}, \quad i = 1, 3,
\end{aligned} \tag{5}$$

where $S_f$ and $I_f$ are the cross-section area and the second moment of the face layers. $E_f$ is the Young's modulus.

As in Refs. [15,16], the behaviour of the core layer is given by a hereditary integral:

$$\begin{aligned}
\sigma_2(x,z,t) &= \int_{-\infty}^{t} Y(t-\tau)\frac{\partial \varepsilon_2(x,z,\tau)}{\partial \tau}\, d\tau = Y^* \frac{\partial \varepsilon_2}{\partial t},\\
\tau_2 &= \frac{Y}{2(1+\nu_c)} * \frac{\partial \gamma_2}{\partial t},
\end{aligned} \tag{6}$$

where $\sigma_2$ and $\tau_2$ are the axial and shear stresses in the core layer, $Y$ is the relaxation function of the material, and $\nu_c$ is the Poisson ratio. $^*$ denotes the classical convolution product. From the strain–displacement relations (3) and the constitutive law (6), the following expressions of the axial force $N_2$, the bending moment $M_2$, and the shear force $T$ in the core layer are obtained:

$$\begin{aligned}
N_2 &= S_c Y^* \left(\frac{\partial^2 u}{\partial x \partial t} + \frac{\partial^2 w}{\partial x \partial t}\frac{\partial w}{\partial x}\right),\\
M_2 &= I_c Y^* \frac{\partial^2 \beta}{\partial x \partial t},\\
T &= \frac{S_c}{2(1+\nu_c)} Y^* \left(\frac{\partial^2 w}{\partial x \partial t} + \frac{\partial \beta}{\partial t}\right),
\end{aligned} \tag{7}$$

where $S_c$ and $I_c$ are the cross-section area and the second moment of the core layer, respectively. For sandwich beams with soft cores, the shear stress is almost constant throughout the thickness of the core layer [2]. Therefore, it is not necessary to introduce a shear correction factor.

The present paper is focused on frequency-domain analyses. In this scope, the constitutive law will be used when the strain is a combination of several harmonics:

$$\varepsilon_2(x,z,t) = \sum_{k=0}^{n}\left(\frac{\varepsilon_2(x,z,k)e^{jk\omega t} + \overline{\varepsilon_2}(x,z,k)e^{-jk\omega t}}{2}\right), \tag{8}$$

where $^{-}$ means the conjugate of a complex number and j is the imaginary unit. In this case, the axial stress can be described by the classical complex Young's modulus representation:

$$\sigma_2(x,z,t)=\sum_{k=0}^{n}\left(\frac{\sigma_2(x,z,k)e^{jk\omega\tau}+\overline{\sigma_2}(x,z,k)e^{-jk\omega\tau}}{2}\right),$$
$$\sigma_2(x,z,k)=E_c(k\omega)\varepsilon_2(x,z,k),$$
$$E_c(k\omega)=jk\omega\int_0^{+\infty}Y(\tau)e^{-jk\omega\tau}\,d\tau, \tag{9}$$

where $E_c$, the complex Young's modulus, is the Fourier transform of the relaxation function. Corresponding expressions can be similarly obtained for the shear stress.

### 2.3. Variational formulation

Using the virtual work principle, a variational formulation of the problem can be written as follows:

$$\delta W_{\text{int}}-\delta W_{\text{ext}}+\delta W_{\text{kin}}=0, \tag{10}$$

where $\delta W_{\text{int}}$, $\delta W_{\text{ext}}$, and $\delta W_{\text{kin}}$ are the virtual works of internal, external, and inertial forces, respectively. The virtual work of internal forces for the whole beam is written by assembling the contributions of each layer:

$$\delta W_{\text{int}}=\sum_{i=1}^{3}\int_0^L N_i\left(\frac{\partial\delta u_i}{\partial x}+\frac{\partial w}{\partial x}\frac{\partial\delta w}{\partial x}\right)dx$$
$$+\int_0^L\left(-(M_1+M_3)\frac{\partial^2\delta w}{\partial x^2}+M^2\frac{\partial\delta\beta}{\partial x}\right)dx+\int_0^L T\left(\frac{\partial\delta w}{\partial x}+\delta\beta\right)dx. \tag{11}$$

Only transverse external forces are considered, and rotational inertia is neglected. Thus, the expressions of $\delta W_{\text{ext}}$ and $\delta W_{\text{kin}}$ are

$$\delta W_{\text{ext}}=\int_0^L F\delta w\,dx \ \text{ with } \ F(x,t)=F_d(x,t)+F_i(t)\delta(x-x_i),$$
$$\delta W_{\text{kin}}=(2\rho_f S_f+\rho_c S_c)\int_0^L\left(\frac{\partial^2 w}{\partial t^2}\delta w+\frac{\partial^2 u}{\partial t^2}\delta u\right)dx, \tag{12}$$

$F_d(x,t)$ and $F_i(t)$ represent, respectively, a distributed force and a concentrated force acting at the point $x=x_i$, $\delta(\cdot)$ is the Dirac delta function, and $\rho_f$ and $\rho_c$ are the densities of the face and core materials. By considering the interface conditions (4), Eq. (10) can be rewritten only in terms of the core variables, i.e., the mid-surface translations $u$ and $w$, and the rotation $\beta$ of the normal to the mid-plan:

$$\int_0^L\left\{N\delta\varepsilon+M_\beta\frac{\partial\delta\beta}{\partial x}-M_w\frac{\partial^2\delta w}{\partial x^2}+T\left(\frac{\partial\delta w}{\partial x}+\delta\beta\right)\right\}dx=\delta W_{\text{ext}}-\delta W_{\text{kin}} \tag{13}$$

with

$$N=N_1+N_2+N_3=2E_fS_f\varepsilon+S_cY^*\frac{\partial\varepsilon}{\partial t},\quad \varepsilon=\frac{\partial u}{\partial x}+\frac{1}{2}\left(\frac{\partial w}{\partial x}\right)^2,$$
$$M_\beta=M_2+\frac{N_1-N_3}{2}h_c=\frac{E_fS_fh_c}{2}\left(h_c\frac{\partial\beta}{\partial x}-h_f\frac{\partial^2 w}{\partial x^2}\right)+I_cY^*\frac{\partial^2\beta}{\partial x\partial t},$$
$$M_w=M_1+M_3+\frac{N_1-N_3}{2}h_f=-E_f\left(2I_f+\frac{S_fh_f^2}{2}\right)\frac{\partial^2 w}{\partial x^2}+\frac{E_fS_fh_ch_f}{2}\frac{\partial\beta}{\partial x},$$
$$T=\frac{S_c}{2(1+\nu_c)}Y^*\left(\frac{\partial^2 w}{\partial x\partial t}+\frac{\partial\beta}{\partial t}\right),\quad \delta\varepsilon=\frac{\partial\delta u}{\partial x}+\frac{\partial w}{\partial x}\frac{\partial\delta w}{\partial x}.$$

## 3. Solution procedure

The solution procedure is based on the harmonic balance technique and the finite element method. Contrary to the common practice in the nonlinear vibration field, the analysis begins with the application of the harmonic balance method. This means that the harmonic balance method is used to transfer the variational formulation (13) into the frequency domain. The variables of the resulting equation are functions only of $x$. Then, a finite element approximation is introduced, leading to a set of algebraic equations that are solved by an arc-length method. Note that the proposed solution procedure allows us to consider the viscoelastic behaviour without any simplification.

### 3.1. Application of the harmonic balance method

Only transverse harmonic excitations are considered:

$$F(x,t)=\frac{F_\omega(x)e^{j\omega t}+\overline{F_\omega}(x)e^{-j\omega t}}{2}. \tag{14}$$

The frequency response is studied by assuming that harmonic transverse motions exist for moderate amplitudes of vibration. The validity of this assumption is discussed in Section 4.1. The transverse displacement and the core rotation are expressed as

$$w(x,t)=\frac{w_\omega(x)e^{j\omega t}+\overline{w_\omega}(x)e^{-j\omega t}}{2},$$
$$\beta(x,t)=\frac{\beta_\omega(x)e^{j\omega t}+\overline{\beta_\omega}(x)e^{-j\omega t}}{2}. \tag{15}$$

With these approximations (15), it can be shown that the axial displacement will contain two harmonic components (0 and $2\omega$) [16]:

$$u(x,t)=u_0(x)+\frac{u_{2\omega}(x)e^{j2\omega t}+\overline{u_{2\omega}}(x)e^{-j2\omega t}}{2}. \tag{16}$$

Similar approximations are used for the virtual displacements:

$$\delta w(x,t)=\frac{\delta w_\omega(x)e^{j\omega t}+\overline{\delta w_\omega}(x)e^{-j\omega t}}{2},$$
$$\delta\beta(x,t)=\frac{\delta\beta_\omega(x)e^{j\omega t}+\overline{\delta\beta_\omega}(x)e^{-j\omega t}}{2},$$
$$\delta u(x,t)=\delta u_0(x)+\frac{\delta u_{2\omega}(x)e^{j2\omega t}+\overline{\delta u_{2\omega}}(x)e^{-j2\omega t}}{2}. \tag{17}$$

Eqs. (14)–(17) are inserted into Eq. (13). Considering the expression of the viscoelastic law in the frequency domain (8)–(9) and integrating over a period of $2\pi/\omega$, a variational equation governing the forced response of the beam is obtained (more details on the derivation of Eq. (18) are given in Appendix A):

$$\int_0^L\left\{2N_0\delta\varepsilon_0+\mathrm{Re}\left(N_{2\omega}\overline{\delta\varepsilon_{2\omega}}+M_{\beta\omega}\frac{\partial\overline{\delta\beta_\omega}}{\partial x}-M_{w\omega}\frac{\partial^2\overline{\delta w_\omega}}{\partial x^2}+T_\omega\left(\frac{\partial\overline{\delta w_\omega}}{\partial x}+\overline{\delta\beta_\omega}\right)\right)\right\}dx$$
$$=\int_0^L\mathrm{Re}(F_\omega\overline{\delta w_\omega})\,dx+(2\rho_fS_f+\rho_cS_c)\omega^2\int_0^L\mathrm{Re}(w_\omega\overline{\delta w_\omega}+4u_{2\omega}\overline{\delta u_{2\omega}})\,dx \tag{18}$$

with

$$N_0=(2E_fS_f+E_c(0)S_c)\varepsilon_0,\quad N_{2\omega}=(2E_fS_f+E_c(2\omega)S_c)\varepsilon_{2\omega},$$
$$\varepsilon_0=\frac{\partial u_0}{\partial x}+\frac{1}{4}\frac{\partial w_\omega}{\partial x}\frac{\partial\overline{w_\omega}}{\partial x},\quad \varepsilon_{2\omega}=\frac{\partial u_{2\omega}}{\partial x}+\frac{1}{4}\left(\frac{\partial w_\omega}{\partial x}\right)^2,$$
$$\delta\varepsilon_0=\frac{\partial\delta u_0}{\partial x}+\frac{1}{2}\mathrm{Re}\left(\frac{\partial w_\omega}{\partial x}\frac{\partial\overline{\delta w_\omega}}{\partial x}\right),\quad \delta\varepsilon_{2\omega}=\frac{\partial\delta u_{2\omega}}{\partial x}+\frac{1}{2}\frac{\partial w_\omega}{\partial x}\frac{\partial\delta w_\omega}{\partial x},$$
$$M_{\beta\omega}=\frac{E_fS_fh_c}{2}\left(h_c\frac{\partial\beta_\omega}{\partial x}-h_f\frac{\partial^2w_\omega}{\partial x^2}\right)+E_c(\omega)I_c\frac{\partial\beta_\omega}{\partial x},$$
$$M_{w\omega}=-E_f\left(2I_f+\frac{S_fh_f^2}{2}\right)\frac{\partial^2w_\omega}{\partial x^2}+\frac{E_fS_fh_ch_f}{2}\frac{\partial\beta_\omega}{\partial x},\quad T_\omega=\frac{E_c(\omega)S_c}{2(1+\nu_c)}\left(\frac{\partial w_\omega}{\partial x}+\beta_\omega\right),$$

where $\mathrm{Re}(\cdot)$ denotes the real part of a complex number. The unknowns of Eq. (18) are the amplitudes $w_\omega(x)$, $\beta_\omega(x)$, $u_{2;}(x)$, and $u_0(x)$.

### 3.2. Finite element model

A two-node element based on formulation (18) is developed in this section. In order to satisfy the continuity requirements, Hermite cubic shape functions are used to approximate the out-of-plane displacement, $w_\omega$, and Lagrange linear shape functions are used for the axial displacements, $u_{2;}$ and $u_0$, and the rotation of the core $\beta_\omega$. Using Hermite polynomials, both the values of the transverse displacement and of its first derivative at the node must be degrees of freedom. Moreover, $w_\omega$, $\beta_\omega$, and $u_{2\omega}$ are complex quantities. Hence, at the element level, each node will have nine degrees of freedom: $u_0$, $u_{2\omega}^R$, $u_{2\omega}^I$, $\beta_\omega^R$, $\beta_\omega^I$, $w_\omega^R$, $w_\omega^I$, $\partial w_\omega^R/\partial x$, and $\partial w_\omega^I/\partial x$ (superscripts $R$ and $I$ denote the real and imaginary parts of a complex number, respectively).

The developed element will be referred to in the rest of the paper as the HBSB (harmonic balance/sandwich beam) element. It has been implemented in the commercial software ABAQUS/Standard using a user element subroutine UEL

[28]. The element assembly procedure gives a set of global equations that can be written symbolically as

$$I(q,\omega)-\omega^2[M]q=F, \tag{19}$$

where $q$ and $F$ are the assembled vector of nodal unknowns and the nodal external force vector, respectively. $[M]$ is a mass matrix (note that $[M]$ is not the standard mass matrix, but rather it results from the discretisation of the second term on the right-hand side of Eq. (18)). $I(q,\omega)$ is the internal force vector, which depends on frequency because materials with frequency-dependent behaviour are considered. In the HBSB model, the complex Young's modulus of the core is given by a tabular function of frequency. The modulus at a given frequency is simply interpolated from this table of data.

The computation of the forced response of a beam is performed in two steps. First, the solution for a fixed frequency is computed by incrementally increasing the amplitude of the excitation force to its prescribed value. Then, the frequency is incremented to obtain the frequency response, keeping the amplitude of the load constant. Response curves of nonlinear systems may have multivalued regions that cannot be obtained by Newton's method alone. Thus, the Riks method, in which the frequency is treated as an additional variable, is used during the second stage of the computations.

## 4. Numerical results and analysis

This section presents numerical examples, which were employed to test the efficiency and the accuracy of the proposed approach. For the computations, a regular mesh that includes 20 HBSB elements was used.

### 4.1. Validation of the HBSB model

#### 4.1.1. Comparison with analyses using direct time integration

Nonlinear transient dynamic computations using direct time integration (Hilbert–Hughes–Taylor scheme) were performed with the ABAQUS/Standard software. A clamped beam under point excitation at the mid-span is studied (Fig. 1). Because of symmetry, only half of the beam was modelled. The core material is assumed to behave as a Kelvin–Voigt solid:

$$\sigma_2=E_0\left(\varepsilon_2+c\frac{\partial\varepsilon_2}{\partial t}\right), \tag{20}$$

where $E_0$ is the storage modulus and $c$ is a parameter that defines the damping. It should be noted that the Kelvin–Voigt model is a particular case of the more general viscoelastic model considered in Section 2.2. Indeed, Eq. (6) reduces to the standard form of the Kelvin–Voigt model (20) when the following relaxation function is considered:

$$Y(t)=E_0\left(1+c\delta(t)\right), \tag{21}$$

where $\delta(\cdot)$ is the Dirac delta function. In the case of periodic motions, the Kelvin–Voigt model leads to the following expression for the complex modulus:

$$E_c(k\omega)=E_0(1+\mathrm{j}ck\omega). \tag{22}$$

Because there is no efficient sandwich beam element available in the ABAQUS element library, the beam was meshed with 8-node plane-stress elements with biquadratic interpolation functions and reduced integration (ABAQUS CPS8R). From a mesh convergence study (not further described here for purposes of brevity), a mesh with 3 elements through the thickness and 111 along the half-length was selected. Also, it was observed that the accuracy of the solution depends strongly on the time step. In order to obtain reliable results, a fixed time step 500 times smaller than the excitation period was employed. In most of the simulations, the beam is initially at rest and is subjected to a harmonic excitation (frequency $\omega$ and load amplitude $F_1$) until a steady-state solution is reached. In that case, when several steady-state solutions exist for the considered excitation, simulations give the solution with the lowest vibration amplitude. In order to obtain the solution with the highest amplitude, the following procedure is used: the computation is started with a higher excitation (frequency $\omega$ and load amplitude $F_2$ with $F_2>F_1$; for the present computations, we have used $F_2=2F_1$). Once a steady-state response is reached, the load amplitude is smoothly decreased to $F_1$. The computation is then continued until a new steady-state solution (corresponding to $F_1$) is reached.

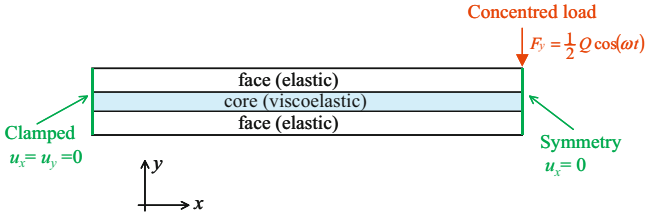


**Fig. 1.** Configuration considered in the simulations using direct time integration.

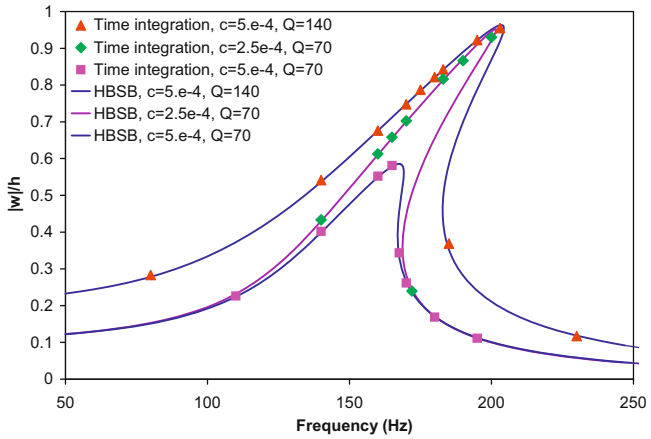


**Fig. 2.** Frequency response curves of a clamped sandwich beam under concentrated harmonic excitation at the centre for several damping parameters ($c$=2.5 × 10$^{-4}$ and 5 × 10$^{-4}$ s) and load amplitudes ($Q$=70 and 140 N): comparison between the HBSB model and direct time integration analyses. The three layers of the beam have a rectangular cross-section with unit width. The following parameters have been considered: $L$=178 × 10$^{-3}$ m, $h_f$=6 × 10$^{-4}$ m, $h_c$=4.5 × 10$^{-5}$ m, $\rho_f$=7,800 kg/m$^3$, $\rho_c$=1200 kg/m$^3$, $E_f$=2.1 × 10$^{11}$ Pa, $\nu_f$=0.3, $E_0$=4.12 × 10$^6$ Pa, and $\nu_c$=0.44.

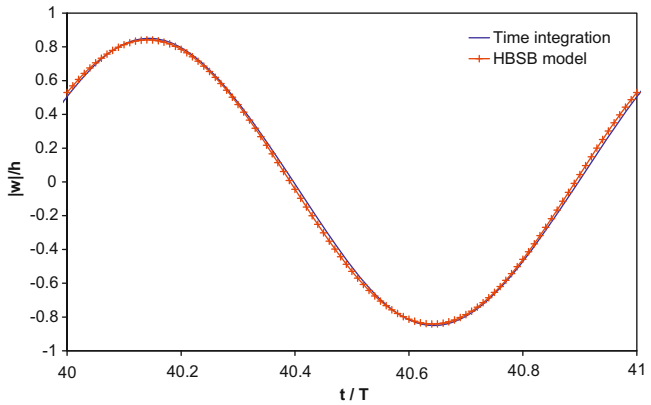


**Fig. 3.** Time response of a clamped beam under excitation at mid-span. The configuration is identical to the one adopted in Fig. 2. The damping parameter of the core material, the amplitude, and the frequency of the excitation are taken as $c$=5 × 10$^{-4}$ s, $Q$=140 N, and $f$=183 Hz, respectively. Note that the time response obtained with the HBSB model is, by assumption, harmonic.

In Fig. 2, results derived from the HBSB model are compared with those of the time-domain analyses. Good agreement is observed between the two methods. The effects of large vibration amplitudes and damping are well predicted by the HBSB model. The analysis of time responses obtained with computations using direct time integration has shown that the first harmonic of the transverse displacement is at least 100 times greater than the other harmonics. Hence, for moderate amplitudes of vibration, higher harmonics have a small influence on the global response of the beam, and the assumption of harmonic deflection is valid (Fig. 3). Of course, for larger amplitudes of vibration, higher harmonics are likely to play a more significant role.

Finally, it should be noted that the HBSB model requires much less computation time than the time domain method. Indeed, the computation of a response curve with the HBSB model on a desktop computer (3 GHz Intel Pentium 4 processor) takes less than 1 min, in contrast to the 3 h required for the time domain method (about 10 simulations at a given frequency are necessary to estimate the frequency response curve, and each simulation takes about 20 min).

### *4.1.2. Comparison with experimental results*

An experimental study of the forced nonlinear vibration of viscoelastic sandwich beams with clamped ends was performed by Kovac et al. [14]. The beam was 0.254 m long and 25.4 mm wide. The face layers were 0.203 mm thick and made of steel. The core was 1.588 mm thick and was composed of a low durometer neoprene. The evolution of the complex modulus of this material is plotted against frequency in Fig. 4. The beam was forced at its centre with an electromagnetic device. Clamped boundary conditions were enforced by inserting the ends of the beam between two steel blocks and then

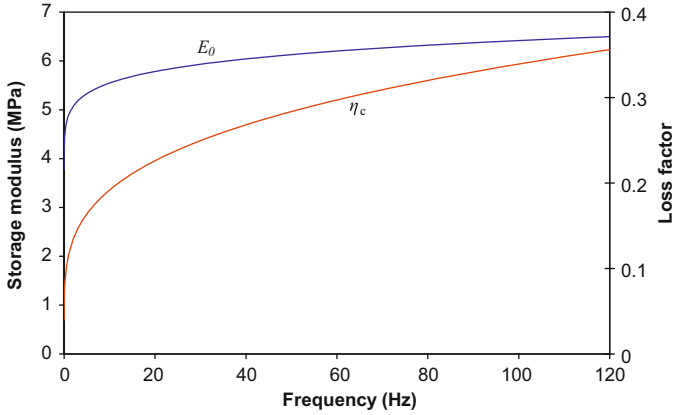


**Fig. 4.** Evolution of the storage modulus $E_0$ with frequency, and the loss factor $\eta_c$ of the low-durometer neoprene used in the work of Kovac et al. [14].

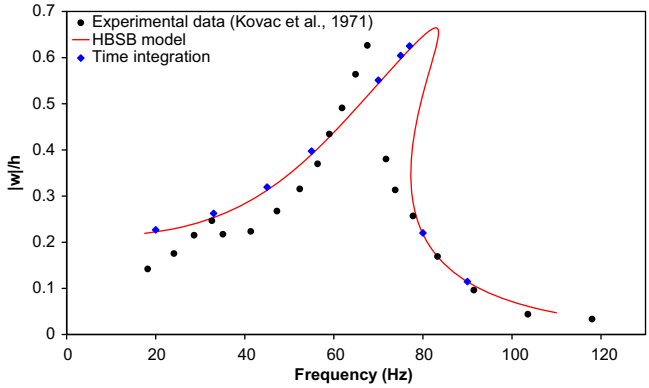


**Fig. 5.** Frequency response curves of a clamped sandwich beam under concentrated harmonic excitation at the centre ($Q$=29.76 N): The HBSB model and direct time integration analyses, compared with the experimental data of Kovac et al. [14].

bolting the blocks. To prevent the crushing of the neoprene layer, the core in the ends of the beam that were in contact with the support mechanism was replaced by aluminium fillers. Moreover, strain gages were mounted on opposite sides of the beam in order to check that the mounting procedure did not induce initial axial load or bending moment. A comparison between the experimental frequency response of Kovac et al. [14], the numerical results obtained with the HBSB model, and the direct time integration analyses is presented in Fig. 5. The configuration considered for the time-domain computations is the one depicted in Fig. 1; the beam was meshed with 381 (3*127) elements. A fairly good agreement between simulation and experiment is observed. The general shapes of the response curves are similar with regard to peak amplitudes and resonant frequencies. However, there are several differences between the experimental and numerical results. First, the numerical curves present a more pronounced hardening-type nonlinearity than the experimental curve. Secondly, a small peak at about 32 Hz is observed experimentally, but this is not predicted by the numerical models. This frequency is about half of the first natural frequency of the beam measured by Kovac et al. [14] (59 Hz). Therefore, this peak is probably due to a 1/2 superharmonic resonance. Of course, the HBSB model cannot describe superharmonic responses, because it is based on the assumption that the transverse displacement is harmonic, as seen in Eq. (15). Time domain simulations are able to deal with multifrequency responses. However, in the present case, no superharmonic resonance is predicted. The exact reason for the discrepancies between simulations and experiments is unknown. However, some possible explanations can be suggested. For example, several studies [20,29,30] have shown that geometric imperfections can have a significant influence on the nonlinear response of thin beams or plates. Geometric imperfections generally reduce the hardening nonlinearity of the frequency response and may even cause a softening-type nonlinearity. Moreover, they may be responsible for the occurrence of superharmonic components in the response [30]. The deviation of the numerical curves near the main resonance would also be due to the axial elasticity of the supports of the experimental setup. Indeed, this elasticity implies that the beam does not stiffen as much as with perfectly rigid supports, leading to a less pronounced hardening nonlinearity of the resonant curve [31]. Finally, it should also be noticed that the force generated by an electromagnetic forcing device may be significantly different from a pure sinusoid. This distortion of the excitation may influence the beam response [32].

### 4.2. Applications

#### 4.2.1. Viscoelastic sandwich beams with constant complex modulus

In the present section, the response of beams with hysteretic damping is analysed. In the case of harmonic vibrations, hysteretic damping produces an energy dissipation that does not depend on frequency and, consequently, the complex Young's modulus is written as [33]

$$E_c(\omega) = E_0\left(1 + \mathrm{j}\eta_c\,\mathrm{sgn}(\omega)\right), \tag{23}$$

where $\eta_c$ is the loss factor and $\mathrm{sgn}(\cdot)$ stands for the signum function. It should be noted that Eq. (23) is not compatible with the viscoelastic law (6) that was used for the derivation of the HBSB model. Therefore, the applicability of Eq. (23) to nonlinear problems should be checked. Because of geometrical nonlinearity, the strain field may contain several harmonic components, even if the beam is subjected to a harmonic excitation. Thus, one must verify that Eq. (23) remains valid for multifrequency responses. A time domain representation of hysteretic damping is [33]

$$\sigma_2(t) = E_0\left(\varepsilon_2(t) - \frac{\eta_c}{\pi}\int_{-\infty}^{+\infty}\frac{\varepsilon_2(\tau)}{(t-\tau)}\,d\tau\right). \tag{24}$$

This model is often referred to as the ideal hysteretic damping model because, in the case of a harmonic strain, it leads to an energy dissipated by cycle that is strictly independent of frequency. A flaw of this model is that it induces a non-causal (anticipatory) behaviour [33,34]. Nevertheless, non-causality is not a concern in the present study because our attention is restricted to steady-state vibrations. By inserting the time-dependence of strain (8) into Eq. (24), $\sigma_2(t)$ can be written in the following form:

$$\sigma_2(x,z,t) = \sum_{k=0}^{n}\left(\frac{\sigma_2(x,z,k)\mathrm{e}^{\mathrm{j}k\omega t} + \overline{\sigma_2}(x,z,k)\mathrm{e}^{-\mathrm{j}k\omega t}}{2}\right)$$
$$\text{with}\quad \sigma_2(x,z,k) = E_0(1 + \mathrm{j}\eta_c\,\mathrm{sgn}(k\omega))\varepsilon_2(x,z,k). \tag{25}$$

This shows that Eq. (23) can be applied when more than one frequency is present.

Fig. 6 shows the linear and nonlinear frequency response curves of a clamped beam under point excitation at quarter-span; the vibration amplitude is measured at the position of the load. A large range of frequencies, which includes the first and second resonances, is considered. One observes that the effect of geometric nonlinearity seems to be more pronounced near the second resonance. Indeed, even if the vibration amplitude reached at the second resonance is about half that at the first resonance, the increase of the resonant frequency due to nonlinearity is about 100 Hz in both cases. It is also interesting to point out that the nonlinear model predicts a greater value of the vibration amplitude at the first resonance than does the linear model. In the following, the amplitudes obtained with the nonlinear and linear models will simply be designated as the nonlinear and linear amplitudes, respectively. Concerning the difference between the nonlinear and linear amplitudes at resonance, the following observations have been made:

- A difference is observed only in the case of clamped beams. Moreover, it depends on the position of the excitation (Fig. 7b). For simply supported beams, the linear and nonlinear amplitudes are identical (Fig. 7a).
- Whereas the mode shape at resonance of a clamped beam depends on the vibration amplitude (Fig. 8b), it does not change when the boundaries are simply supported (Fig. 8a). Note that similar behaviour has already been observed in the case of thin homogeneous beams [23,35,36] and plates [37,38].

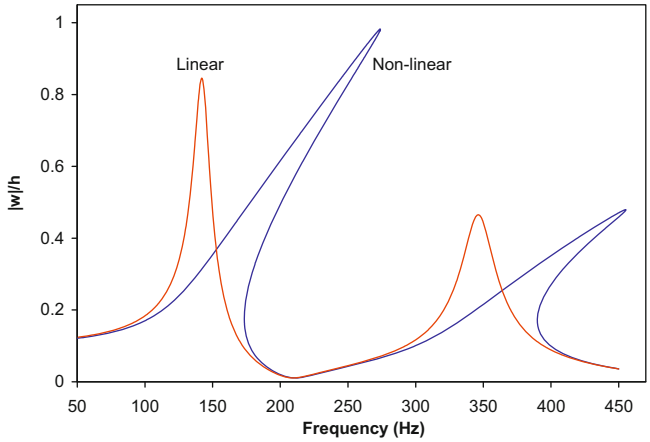


**Fig. 6.** Response curves of a clamped sandwich beam subjected to a harmonic concentrated force ($Q$=150 N) at quarter-span. The loss factor of the core material is $\eta_c$=0.25. Other data are those of Fig. 2.

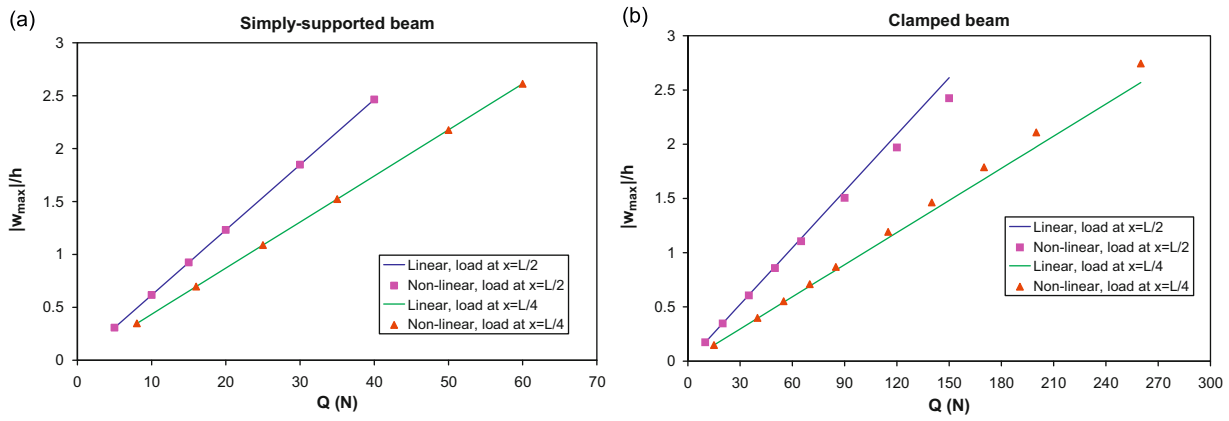


**Fig. 7.** Maximum vibration amplitude reached at the first resonance as a function of the amplitude of the excitation. Concentrated forces at mid-span and at quarter-span are considered: (a) simply supported beam with immovable ends and (b) clamped beam. Data are those of Fig. 6.

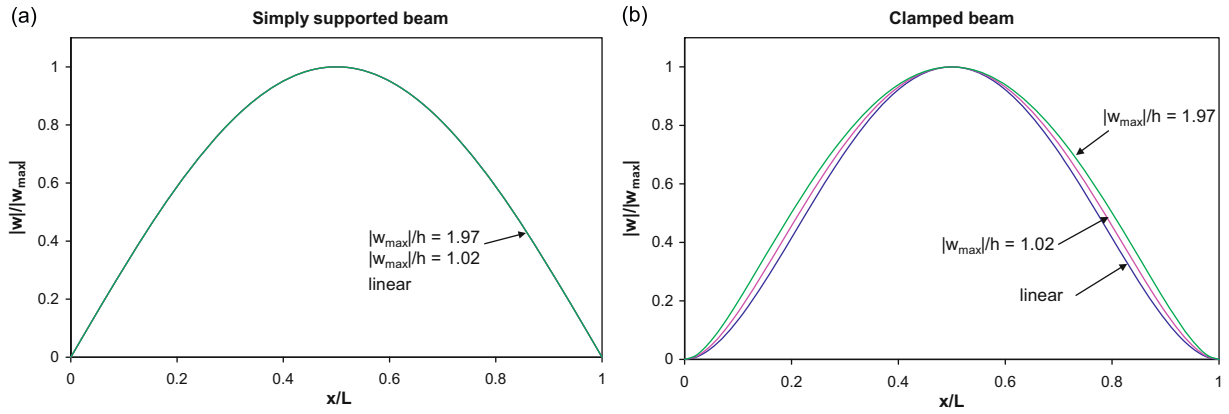


**Fig. 8.** Effect of the vibration amplitude on the first mode: (a) simply supported beam with immovable ends; the mode shape does not change and (b) clamped beam. Data are as in Fig. 6.

- The analytical model proposed in Ref. [16], which is based on the one-mode Galerkin's method (where the change in mode shape is not taken into account), predicts the same amplitude in both the linear and nonlinear cases.

From these observations, one concludes that the difference between the nonlinear and linear amplitudes is related to the change of the mode shape. In order to understand this phenomenon, let us consider the energy balance for the sandwich beam. Because the core layer experiences predominantly shear deformations, the average power $P_D$ dissipated in the beam during a cycle can be estimated by

$$P_D = \frac{E_0 S_c \eta_c \omega}{4(1+\nu_c)} \int_0^L |\gamma_\omega|^2 \, dx, \tag{26}$$

where $\gamma_\omega$ is the amplitude of the shear strain in the core layer, given by

$$\gamma_\omega = \frac{\partial w_\omega}{\partial x} + \beta_\omega. \tag{27}$$

The average power $P_W$ of the external force can be written as

$$P_W = -\frac{\omega}{2} Q_A w^I_{\omega A}, \tag{28}$$

where $Q_A$ is the amplitude of the load, which is assumed to be real, and $w^I_{\omega A}$ is the imaginary part of the displacement at the load position. By setting the power dissipated equal to the power of the external load, a relationship between the maximal vibration amplitude $|w_{\max}|$ and the load amplitude is obtained:

$$\frac{|w_{\max}|}{Q_A} = \frac{2(1+\nu_c)}{E_0 \eta_c L} \frac{N_W}{N_D} \tag{29}$$

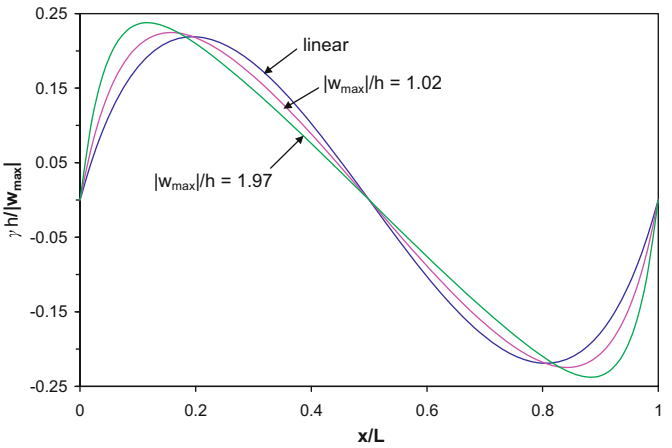


**Fig. 9.** Distribution of shear strain associated with the first mode of a clamped sandwich beam for several values of the vibration amplitude. Configuration and material parameters are those of Fig. 6.

**Table 1**
Values of the numbers $N_D$ and $N_W$, Eq. (29), corresponding to the first mode of a clamped sandwich beam for several values of the vibration amplitude. Configuration and material parameters are identical to those adopted in Fig. 8b.

| $\|w_{max}\|/h$ | $N_D$ | Load at $x=L/2$ | | Load at $x=L/4$ | |
|---|---|---|---|---|---|
| | | $N_W$ | $N_W/N_D$ | $N_W$ | $N_W/N_D$ |
| Linear | 0.726 | 1 | 1.38 | 0.567 | 0.78 |
| 1.02 | 0.742 | 1 | 1.35 | 0.604 | 0.81 |
| 1.97 | 0.772 | 1 | 1.30 | 0.642 | 0.83 |

with

$$N_D = \frac{S_c}{|w_{\max}|^2 L}\int_0^L |\gamma_\omega|^2\,dx \quad \text{and} \quad N_W = -\frac{w^I_{\omega A}}{|w_{\max}|}.$$

$N_D$ is a dimensionless number that characterizes the effect of the variation in mode shape on the dissipation of energy in the viscoelastic layer. This effect is due to the fact that the distribution of shear strain changes with the mode shape (Fig. 9). The number $N_W$ quantifies the effect of the mode shape on the power of the external load. Of course, these two numbers are constant when the mode shape does not depend on the vibration amplitude. As mentioned previously, this situation occurs with simply supported beams. Therefore, in this case, the vibration amplitude at resonance is proportional to the amplitude of the load (Fig. 7a).

The values of the numbers $N_D$ and $N_W$ corresponding to the first mode of a clamped beam are given in Table 1 for several amplitudes of vibration. It is observed that $N_D$ increases with the vibration amplitude. This means that, for the considered configuration, the change of the mode shape enhances the dissipation of energy in the viscoelastic layer. The evolution of $N_W$ with the vibration amplitude depends on the position of the load. When the load is applied at the centre of the beam, i.e., where the deflection is at a maximum, $N_W$ does not depend on the vibration amplitude. Hence, in this case, the variation of the mode shape has no effect on the power of the external load, whereas it enhances energy losses due to damping. That is the reason why, for the beam loaded at mid-span, the nonlinear amplitude of vibration at resonance is lower than the linear one (Fig. 7b). When the load is applied at quarter-span, $N_W$ increases with the vibration amplitude, indicating that the power of the external load is enhanced by the change in the mode shape. Furthermore, the rate of increase of $N_W$ is greater than that of $N_D$. Therefore, in this case, the nonlinearity induces an increase in the vibration amplitude at resonance (Fig. 7b).

*4.2.2. Sandwich beam with frequency-dependent behaviour*

In this section, the response of a simply supported beam, whose core modulus depends strongly on frequency, is investigated. The considered core material is a polypropylene; Fig. 10 shows the evolution of its storage modulus and loss factor with frequency at 30 and 60 °C. The linear and nonlinear frequency response curves of the beam are plotted in Fig. 11. One sees that the vibration amplitude at resonance varies strongly with temperature. The maximum amplitude is larger at 60 °C, because the material loss factor is smaller at this temperature. Also, the effect of temperature appears to be more pronounced in the nonlinear case. Indeed, whereas both models predict about the same maximum amplitude of vibration at 30 °C, the nonlinear amplitude is 23% greater than the linear one at 60 °C. Because a simply supported beam is

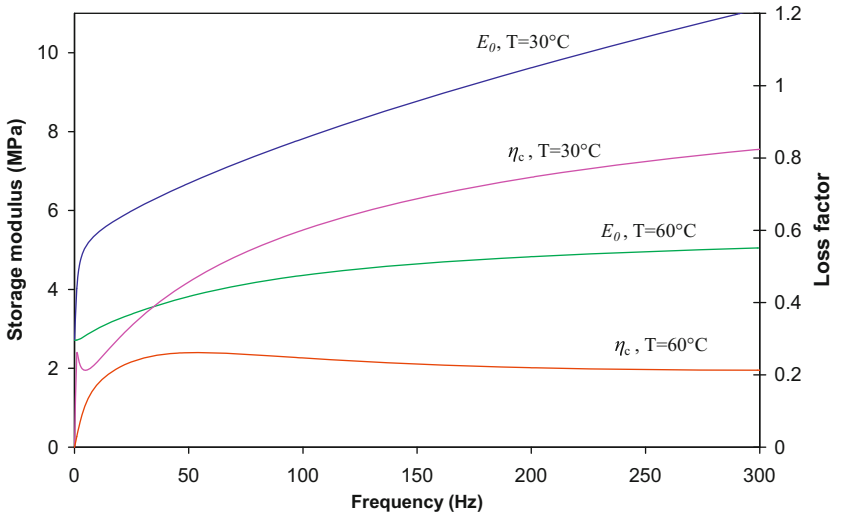


**Fig. 10.** Evolution of the storage modulus $E_0$ with frequency and the loss factor $\eta_c$ of polypropylene at 30 and 60 °C.

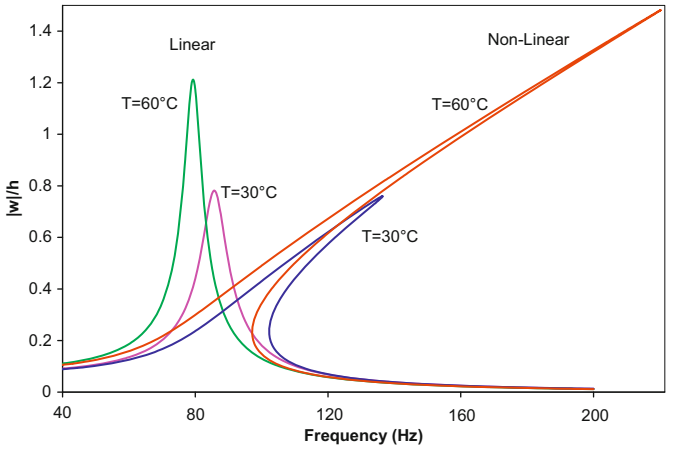


**Fig. 11.** Response curves of a simply supported beam with immovable ends subjected to a concentrated load ($Q$=20 N) at mid-span at 30 and 60 °C. Frequency-dependent material behaviour (Fig. 10). Other data are those of Fig. 7.

considered, this phenomenon cannot be attributed to a change of the mode shape. Instead, it is related to the frequency dependence of the core modulus. When geometrically nonlinear effects are taken into account, the increase of the vibration amplitude, resulting from the change of temperature, generates an increase in the resonance frequency. Consequently, because the core material has a frequency-dependent behaviour, the change in the material properties is larger than in the linear case, leading to a more pronounced effect for temperature.

*4.2.3. Sandwich beam with initial axial strain*

We now investigate the effect of an initial axial strain $\varepsilon_0$ on the response of a beam. For this purpose, a constant axial displacement, $u_0(L)=L\,\varepsilon_0$, is applied at one end of the beam. Frequency-response curves obtained for several values of $\varepsilon_0$ are depicted in Fig. 12. One observes that the hardening nonlinearity of the beam response is reduced when a tensile pre-strain is applied. A compressive strain gives the opposite effect. The hardening-type behaviour of beams is induced by the in-plane stretching that arises when the vibration amplitude increases. It is therefore somewhat surprising that a tensile axial pre-strain leads to a less marked nonlinearity. The effect of an axial pre-strain can be explained by considering the nonlinear vibration of a thin, elastic, initially strained beam. In this case, the following expression for the resonance frequency can be obtained by using the one-mode Galerkin's method:

$$\left(\frac{\omega}{\omega_L}\right)^2 = 1+\frac{3}{4}\frac{k_{nl}}{k}A^2 \tag{30}$$

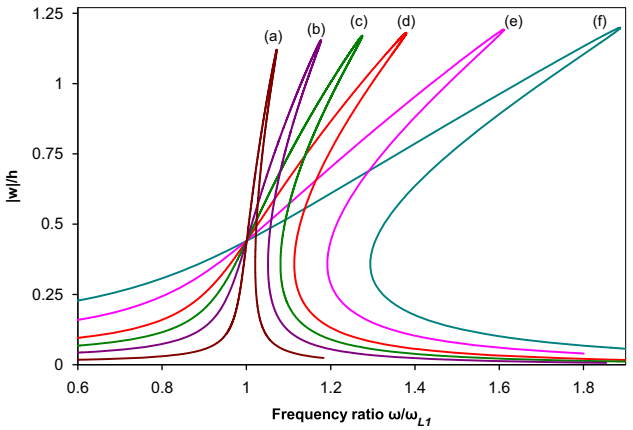


**Fig. 12.** Effect of an initial axial strain $\varepsilon_0$ on the frequency response of a clamped beam under point excitation ($Q$=70 N) at mid-span: (a) $\varepsilon_0=6.74\times10^{-4}$; (b) $\varepsilon_0=2.25\times10^{-4}$; (c) $\varepsilon_0=1.12\times10^{-4}$; (d) $\varepsilon_0=5.62\times10^{-5}$; (e) $\varepsilon_0=0$; and (f) $\varepsilon_0=-2.81\times10^{-5}$. Data are as in Fig. 6.

with

$$k=ES\varepsilon_0\int_0^L\left(\frac{\partial W}{\partial x}\right)^2dx+EI\int_0^L\left(\frac{\partial^2 W}{\partial x^2}\right)^2dx \quad \text{and} \quad k_{\mathrm{nl}}=\frac{ES}{2L}\left[\int_0^L\left(\frac{\partial W}{\partial x}\right)^2dx\right]^2,$$

where $E$ is the Young's modulus; $S$ and $I$ are the area and the second moment of the beam cross-section, respectively; $A$ is the vibration amplitude; $\omega_L$ is the linear natural frequency; and $W(x)$ is a trial function that approximates the transverse displacement. $k$ and $k_{\mathrm{nl}}$ are linear and nonlinear modal stiffness coefficients. One observes that the nonlinear stiffness coefficient $k_{\mathrm{nl}}$ does not depend on the axial pre-strain. Thus, when a tensile strain is prescribed, only the linear stiffness $k$ increases and therefore the weight of the nonlinear term is reduced, leading to a less marked hardening-type behaviour.

## 5. Conclusions

A computational model for the analysis of forced nonlinear vibrations of viscoelastically damped sandwich beams is proposed. A zig-zag model is used to describe the beam kinematics. An efficient solution procedure, based on the harmonic balance technique and the finite element method, allows one to compute the nonlinear response in any range of frequencies with a low computation load. The accuracy of the proposed strategy has been established, at least for moderate amplitudes of vibration, through comparison with the results of fully nonlinear dynamic simulations using direct time integration and with experimental data.

The proposed model has permitted us to study the effect of large vibration amplitudes on the damping properties of sandwich beams. It has been observed that, in the nonlinear regime, the amplitude of vibration at resonance is in general different from the one predicted by a linear model. This phenomenon is due to the change of the mode shape with the vibration amplitude and, when materials having a frequency-dependent behaviour are considered, to the increase of the resonance frequency with the amplitude of vibration. Moreover, it has been shown that an initial axial strain has a significant influence on the effect of nonlinearity. A tensile strain induces a less-pronounced hardening-type behaviour.

Future work will be focused on extending the model to three-dimensional geometries and multifrequency vibrations.

## Acknowledgements

This work was supported by the European Community through the FP6 STREP project CASSEM (Composite and Adaptive Structures: Simulation, Experimentation, and Modelling), Contract no. 013517. The authors also thank Dr. N. Moustaghfir for helpful discussions.

## Appendix A. Derivation of the frequency domain formulation (18)

Eq. (18) results from the application of the harmonic balance method to the virtual work principle equation (13). The term associated with the axial force, $N\delta\varepsilon$, is first considered. Using approximations (15)–(16), it can be easily shown that the axial strain and the virtual strain contain harmonics 0 and $2\omega$:

$$\varepsilon(x,t)=\varepsilon_0(x)+\frac{\varepsilon_{2\omega}(x)\mathrm{e}^{\mathrm{j}2\omega t}+\overline{\varepsilon_{2\omega}}(x)\mathrm{e}^{-\mathrm{j}2\omega t}}{2},$$

$$\delta\varepsilon(x,t)=\delta\varepsilon_0(x)+\frac{\delta\varepsilon_{2\omega}(x)\mathrm{e}^{\mathrm{j}2\omega t}+\overline{\delta\varepsilon_{2\omega}}(x)\mathrm{e}^{-\mathrm{j}2\omega t}}{2}. \tag{A.1}$$

By considering the expression for the axial force, $N=2E_fS_f\varepsilon+S_cY^*(\partial\varepsilon/\partial t)$, and the constitutive relations (5)–(9), the time evolution of $N$ can be written as

$$N(x,t)=N_0(x)+\frac{N_{2\omega}(x)\mathrm{e}^{\mathrm{j}2\omega t}+\overline{N_{2\omega}}(x)\mathrm{e}^{-\mathrm{j}2\omega t}}{2} \tag{A.2}$$

with

$$N_0=(2E_fS_f+E_c(0)S_c)\varepsilon_0 \quad \text{and} \quad N_{2\omega}=(2E_fS_f+E_c(2\omega)S_c)\varepsilon_{2\omega}.$$

Therefore, the virtual work of the axial force can be written as

$$N\delta\varepsilon=N_0\delta\varepsilon_0+\tfrac{1}{2}\mathrm{Re}(N_{2\omega}\overline{\delta\varepsilon_{2\omega}})+\text{harmonic terms}. \tag{A.3}$$

The harmonic terms disappear after integration over a period, and thus:

$$\frac{2}{T'}\int_0^{T'}(N\delta\varepsilon)\,dt=2N_0\delta\varepsilon_0+\mathrm{Re}(N_{2\omega}\overline{\delta\varepsilon_{2\omega}}), \tag{A.4}$$

where $T'=2\pi/\omega$.

The second term, $M_\beta(\partial\delta\beta/\partial x)$, is now considered. Moment $M_\beta$ is given by

$$M_\beta=\frac{E_fS_fh_c}{2}\left(h_c\frac{\partial\beta}{\partial x}-h_f\frac{\partial^2w}{\partial x^2}\right)+I_cY^*\frac{\partial^2\beta}{\partial x\partial t}. \tag{A.5}$$

Because $M_\beta$ depends linearly on $w$ and $\beta$, with the assumed temporal dependence of the displacement vector (15), $M_\beta$ only contains the first harmonic:

$$M_\beta(x,t)=\frac{M_{\beta\omega}(x)\mathrm{e}^{\mathrm{j}\omega t}+\overline{M_{\beta\omega}}(x)\mathrm{e}^{-\mathrm{j}\omega t}}{2} \tag{A.6}$$

with

$$M_{\beta\omega}=\frac{E_fS_fh_c}{2}\left(h_c\frac{\partial\beta_\omega}{\partial x}-h_f\frac{\partial^2w_\omega}{\partial x^2}\right)+E_c(\omega)I_c\frac{\partial\beta_\omega}{\partial x}.$$

To obtain the last term of the expression of $M_{\beta\omega}$, the relationship between the convolution product and complex Young's modulus has been used (see Section 2.2). With the use of Eq. (17), the virtual work of $M_\beta$ can be expressed as

$$M_\beta\frac{\partial\delta\beta}{\partial x}=\frac{1}{4}\left(M_{\beta\omega}\frac{\partial\overline{\delta\beta_\omega}}{\partial x}+\overline{M_{\beta\omega}}\frac{\partial\delta\beta_\omega}{\partial x}\right)+\text{harmonic terms}. \tag{A.7}$$

The harmonic terms vanish after integration over a period:

$$\frac{2}{T'}\int_0^{T'}\left(M_\beta\frac{\partial\delta\beta}{\partial x}\right)dt=\mathrm{Re}\left(M_{\beta\omega}\frac{\partial\overline{\delta\beta_\omega}}{\partial x}\right). \tag{A.8}$$

Similarly, it can be shown that

$$\begin{gathered}\frac{2}{T'}\int_0^{T'}\left(M_w\frac{\partial^2\delta w}{\partial x^2}\right)dt=\mathrm{Re}\left(M_{w\omega}\frac{\partial^2\overline{\delta w_\omega}}{\partial x^2}\right),\\ \frac{2}{T'}\int_0^{T'}(\delta W_{\mathrm{ext}}-\delta W_{\mathrm{kin}})\,dt=\mathrm{Re}\left(F_\omega\overline{\delta w_\omega}+(2\rho_fS_f+\rho_cS_c)\omega^2(w_\omega\overline{\delta w_\omega}+4u_{2\omega}\overline{\delta u_{2\omega}})\right),\\ \frac{2}{T'}\int_0^{T'}\left(T\left(\frac{\partial\delta w}{\partial x}+\delta\beta\right)\right)dt=\mathrm{Re}\left(T_\omega\left(\frac{\partial\overline{\delta w_\omega}}{\partial x}+\overline{\delta\beta_\omega}\right)\right).\end{gathered} \tag{A.9}$$

Eqs. (A.4), (A.8), and (A.9) allow us to obtain the frequency-domain formulation (18).

## References

[1] E.M. Kerwin, Damping of flexural waves by a constrained viscoelastic layer, *Journal of the Acoustical Society of America* 31 (1959) 952–962.
[2] H. Hu, S. Belouettar, M. Potier-Ferry, E.M. Daya, Review and assessment of various theories for modelling sandwich composites, *Composite Structures* 84 (3) (2008) 282–292.
[3] R.A. DiTaranto, Theory of vibratory bending for elastic and viscoelastic layered finite beams, *Journal of Applied Mechanics* 87 (1965) 881–886.
[4] R.A. DiTaranto, W. Blasingame, Composite damping of vibrating sandwich beams, *Journal of Engineering for Industry* 89 (1967) 633–638.
[5] D.J. Mead, S. Markus, The forced vibration of three-layer damped sandwich beams with arbitrary boundary conditions, *Journal of Sound and Vibration* 10 (2) (1969) 163–175.
[6] M.J. Yan, E.H. Dowell, Governing equations for vibrating constrained-layer damping sandwich plates and beams, *Journal of Applied Mechanics* 94 (1972) 1041–1046.

[7] D.K. Rao, Frequency and loss factors of sandwich beams under various boundary conditions, *Journal of Mechanical Engineering Sciences* 20 (5) (1978) 271–282.
[8] M.L. Soni, Finite element analysis of viscoelastically damped structures, *Shock and Vibration Bulletin* 51 (1) (1981) 97–105.
[9] P. Cupial, J. Niziol, Vibration and damping analysis of a three-layered composite plate with a viscoelastic mid-layer, *Journal of Sound and Vibration* 183 (1) (1995) 99–114.
[10] T.C. Ramesh, N. Ganesan, Finite element analysis of conical shells with a constrained viscoelastic layer, *Journal of Sound and Vibration* 171 (5) (1994) 577–601.
[11] T.T. Baber, R.A. Maddox, C.E. Orozco, A finite element model for harmonically excited viscoelastic sandwich beams, *Computers and Structures* 66 (1) (1998) 105–113.
[12] E.M. Daya, M. Potier-Ferry, A shell finite element for viscoelastically damped sandwich structures, *Revue Européenne des Eléments Finis* 11 (1) (2002) 39–56.
[13] L. Duigou, E.M. Daya, M. Potier-Ferry, Iterative algorithms for non-linear eigenvalue problems. Application to vibrations of viscoelastic shells, *Computer Methods in Applied Mechanics and Engineering* 192 (11–12) (2003) 1323–1335.
[14] E.J. Kovac, W.J. Anderson, R.A. Scott, Forced non-linear vibrations of a damped sandwich beam, *Journal of Sound and Vibration* 17 (1) (1971) 25–39.
[15] M.W. Hyer, W.J. Anderson, R.A. Scott, Non-linear vibrations of three-layer beams with viscoelastic cores, I. Theory, *Journal of Sound and Vibration* 46 (1) (1976) 121–136.
[16] E.M. Daya, L. Azrar, M. Potier-Ferry, An amplitude equation for the non-linear vibration of viscoelastically damped sandwich beams, *Journal of Sound and Vibration* 271 (3–5) (2004) 789–813.
[17] X. Zhang, A.G. Erdman, Dynamic responses of flexible linkage mechanisms with viscoelastic constrained layer damping treatment, *Computers and Structures* 79 (13) (2001) 1269–1274.
[18] A.C. Galucio, J.-F. Deü, R. Ohayon, Hybrid active–passive damping treatment of sandwich beams in non-linear dynamics, *Journal of Vibration and Control* 13 (7) (2007) 851–881.
[19] L. Azrar, E.H. Boutyour, M. Potier-Ferry, Non-linear forced vibrations of plates by an asymptotic-numerical method, *Journal of Sound and Vibration* 252 (4) (2002) 657–674.
[20] F. Perignon, Vibrations Forcées de Structures Minces, Elastiques, Non-linéaires, Ph.D. Thesis, University of Aix-Marseille II, 2004.
[21] R. Lewandowki, Computational formulation for periodic vibration of geometrically nonlinear structures (parts I and II), *International Journal of Solids and Structures* 34 (15) (1997) 1929–1964.
[22] P. Ribeiro, M. Petyt, Non-linear vibration of plates by the hierarchical finite element and continuation methods, *International Journal of Mechanical Sciences* 41 (4–5) (1999) 437–459.
[23] P. Ribeiro, M. Petyt, Non-linear vibration of beams with internal resonance by the hierarchical finite-element method, *Journal of Sound and Vibration* 224 (4) (1999) 591–624.
[24] V.P. Iu, Y.K. Cheung, S.L. Lau, Non-linear vibration analysis of multilayer beams by incremental finite elements (parts I and II), *Journal of Sound and Vibration* 100 (3) (1985) 359–382.
[25] V.P. Iu, Y.K. Cheung, Non-linear vibration analysis of multilayer sandwich plates by incremental finite elements (parts I and II), *Engineering Computations* 3 (1986) 36–52.
[26] E. Carrera, S. Brischette, A survey with numerical assessment of classical and refined theories for the analysis of sandwich plates, *Applied Mechanics Reviews* 62 (1) (2009) 010803.
[27] W.S. Burton, A.K. Noor, Assessment of computational models for sandwich panels and shells, *Computer Methods in Applied Mechanics and Engineering* 124 (1995) 125–151.
[28] *ABAQUS Documentation (Version 6.5)*, ABAQUS Inc, 2004.
[29] M. Amabili, Theory and experiments for large-amplitude vibrations of rectangular plates with geometric imperfections, *Journal of Sound and Vibration* 291 (2006) 539–565.
[30] M. Amabili, S. Carra, Thermal effects on geometrically nonlinear vibrations of rectangular plates with fixed edges, *Journal of Sound and Vibration* 321 (2009) 936–954.
[31] J.A. Bennett, J.G. Eisley, A multiple degree-of-freedom approach to nonlinear beam vibrations, *AIAA Journal* 8 (4) (1970) 734–739.
[32] G.R. Tomlinson, Force distortion in resonance testing of structures with electro-dynamic vibration exciters, *Journal of Sound and Vibration* 63 (1979) 337–350.
[33] G. Muscolino, A. Palmeri, F. Ricciardelli, Time-domain response of linear hysteretic systems to deterministic and random excitations, *Earthquake Engineering and Structural Dynamics* 34 (2005) 1129–1147.
[34] G.B. Muravskii, Linear models with nearly frequency independent complex stiffness leading to causal behaviour in time domain, *Earthquake Engineering and Structural Dynamics* 36 (2007) 13–33.
[35] L. Azrar, R. Benamar, R.G. White, A semi-analytical approach to the non-linear dynamic response of beams at large amplitudes, part II: multimode approach to the steady state forced periodic response, *Journal of Sound and Vibration* 255 (1) (2002) 1–41.
[36] R. Benamar, M.M.K. Bennouna, R.G. White, The effects of large vibration amplitudes on the mode shapes and natural frequencies of thin elastic structures—part I: simply supported and clamped–clamped beams, *Journal of Sound and Vibration* 149 (2) (1991) 179–195.
[37] P. Ribeiro, M. Petyt, Non-linear free vibration of isotropic plates with internal resonance, *International Journal of Non-linear Mechanics* 35 (2) (2000) 263–278.
[38] P. Ribeiro, Nonlinear vibrations of simply-supported plates by the *p*-version finite element method, *Finite Elements in Analysis and Design* 41 (9–10) (2005) 911–924.